

Balancing Generalization and Specialization in Zero-shot Learning

Yun Li^{1*}, Zhe Liu¹, Lina Yao¹ and Xiaojun Chang²

¹University of New South Wales

²University of Technology Sydney

{yun.li5, zhe.liu4, lina.yao}@unsw.edu.au, cxj273@gmail.com

Abstract

Zero-Shot Learning (ZSL) aims to transfer classification capability from seen to unseen classes. Recent methods have proved that generalization and specialization are two essential abilities to achieve good performance in ZSL. However, they all focus on only one of the abilities, resulting in models that are either too general with the degraded classifying ability or too specialized to generalize to unseen classes. In this paper, we propose an end-to-end network with balanced generalization and specialization abilities, termed as BGSNet, to take advantage of both abilities, and balance them at instance- and dataset-level. Specifically, BGSNet consists of two branches: the Generalization Network (GNet), which applies episodic meta-learning to learn generalized knowledge, and the Balanced Specialization Network (BSNet), which adopts multiple attentive extractors to extract discriminative features and fulfill the instance-level balance. A novel self-adjusting diversity loss is designed to optimize BSNet with less redundancy and more diversity. We further propose a differentiable dataset-level balance and update the weights in a linear annealing schedule to simulate network pruning and thus obtain the optimal structure for BSNet at a low cost with dataset-level balance achieved. Experiments on four benchmark datasets demonstrate our model’s effectiveness. Sufficient component ablations prove the necessity of integrating generalization and specialization abilities.

1 Introduction

Humans can easily accumulate past knowledge to perceive novel concepts. Inspired by this, Zero-Shot Learning (ZSL) is proposed to perform inference over novel classes whose samples are unseen during training. The bridge between seen and unseen classes is the shared semantic attributes that describe the visual appearance, e.g., *grey wings*. A more rigorous extension of ZSL is Generalized Zero-Shot Learning (GZSL), which further requires to retain the ability to classify seen

classes. A typical schema of ZSL/GZSL is to learn the visual representations from images, project visual and semantic embeddings to a common space, and then perform nearest neighbor search in the space for classification [Zhu *et al.*, 2019; Xu *et al.*, 2020; Gao *et al.*, 2020; Li *et al.*, 2021].

Reviewing these successful methods, we find that the abilities of generalization, i.e., how well the learned representation can be transferred to unseen classes, and specialization, i.e., extracting discriminative features, are two principles that lead to good performance. Targeting on better generalization, recent works explore meta-learning to learn more generalized knowledge [Li *et al.*, 2021; Liu *et al.*, 2021], or implicitly learn semantic-visual correlations on unseen classes by synthesizing unseen samples [Gao *et al.*, 2020; Zhang *et al.*, 2021]. With generalization ability, models can transfer knowledge to unseen classes. But to classify images, specialization is indispensable. Some efforts adopt attention mechanisms to extract discriminative features [Xie *et al.*, 2019; Huynh and Elhamifar, 2020], or localize distinct regions by semantic guidance [Xu *et al.*, 2020; Zhu *et al.*, 2019].

However, few of them consider the two abilities simultaneously, causing their models to be either too general to classify highly-similar images or too specialized and thus overfit seen class. This problem exists not only at the instance level, i.e., when classifying a specific image, but also at the dataset level. For example, AwA2 and SUN are two widely-used ZSL benchmark datasets, containing 32 coarse-grained and 712 fine-grained classes, respectively. Intuitively, AwA2 has a higher demand for generalized knowledge, while SUN requires a model that strengthens discriminative features. Some studies paved the way to adopt Neural Network Search (NAS) to find the dataset-specific optimal network structure [Min *et al.*, 2020; Yan *et al.*, 2021]. However, NAS is expensive and slow, making NAS usage not practical.

To address the above problems, we propose a two-branch network, dubbed BGSNet, to equip generalization and specialization abilities at the same time, and to balance the two abilities at instance- and dataset-level at a low cost. The two branches are Generalization Network (GNet), which adopts episodic meta-learning to learn transferable knowledge, and Balanced Specialization Network (BSNet), composed of multiple attentive feature extractors focusing on discriminative visual information. Unlike existing methods, we generate attentive weights based on both generalized and specialized

*Contact Author

visual embeddings. Thus the attention can enhance distinctive features and also balance the two abilities by adjusting weights of BSNet. We design a dynamic diversity loss to optimize instance-level balance. This novel loss is self-adjusting based on weight distributions of visual channels and BSNet sub-modules. It has a self-calculated margin to adjust the optimization purposes during training, and ultimately reduce redundancy and increase specialization diversity. Additionally, we apply differentiable dataset-level weights to further balance the two abilities. The dataset-level weights are updated in a linear annealing schedule and will finally be binarized to simulate network pruning. Thus it can find the approximate best network structure without extra computations.

In summary, we make the following contributions:

- We present BGSNet for ZSL/GZSL. BGSNet combines and balances generalization and specialization abilities to retain the discrimination power and provide enough flexibility to learn novel concepts.
- We design a dynamic diversity loss to avoid channel and modular redundancy and increase diversity. We also prove its correctness theoretically and effectiveness experimentally.
- We fulfill dataset-level balance between generalization and specialization, and utilize the balance to find optimal dataset-specific architecture, which avoids the high-cost of NAS.
- We conduct extensive experiments on four benchmark datasets in both ZSL and GZSL settings, and BGSNet consistently outperforms or perform comparable to the SOTA.

2 Method

Suppose that training data $\mathcal{S} = \{(x, y, a) | x \in X^S, y \in Y^S, a \in A^S\}$ from seen classes (classes with labeled samples) are given, where $x \in X^S$ is an image with its label $y \in Y^S$, and $a \in A^S$ represents the corresponding attribute (or other semantic information) of class y . For ZSL, given test set $\mathcal{U} = \{(x, y, a) | x \in X^U, y \in Y^U, a \in A^U\}$ from unseen classes, we aim to predict the label $y \in Y^U$ for each image $x \in X^U$. The class sets of training and testing are disjoint, i.e., $Y^S \cap Y^U = \emptyset$. Meanwhile, for GZSL, testing images can be from seen and unseen classes, i.e., $\mathcal{Y} = Y^S \cup Y^U$.

2.1 Overview.

As Figure 1 shows, BGSNet consists of two branches: the Generalization Net (GNet) and the Balanced Specialization Net (BSNet). GNet (§ 2.2) adopts meta-learning to learn more generalized knowledge that is commonly shared across classes and can be easily transferred to unseen classes. BSNet (§ 2.3) maximizes the specialization capability to discover discriminative features for classification. It also balances the generalization and specialization abilities of BGSNet by adjusting the weights of BSNet at the instance- and dataset-level. The dataset-level weights also play a role in automatically finding the best network structure of BSNet in a linear annealing schedule. Both branches are trained with classification loss (L_g and L_s , respectively). An additional diversity loss L_{div} is proposed to optimize the instance-level weights across sub-modules BSN_i in BSNet to enrich the diversity.

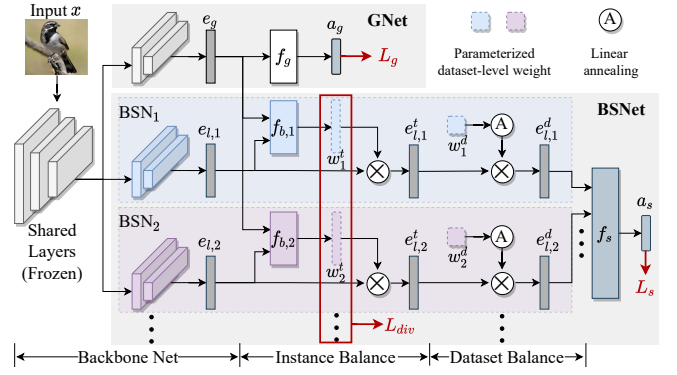


Figure 1: Overview of BGSNet. BGSNet has two branches: GNet and BSNet. For GNet, the input image x is fed into the Backbone Net to extract the visual embedding e_g . Then, the predictor f_g embeds e_g to the semantic space as a_g . For BSNet, x is passed through N sub-modules $\{BSN_i\}_{i=1}^N$, where visual extraction, instance- and dataset-level balancing are performed. BSN_i shares most backbone layers with GNet while adopting different tail layers to extract specialized visual embedding $e_{l,i}$. $e_{l,i}$ and e_g are further used to generate weights w_i^t to conduct instance-level balancing. Then, dataset-level balancing is performed by using parameterized weight w_i^d in a linear annealing schedule. All the balanced embeddings $e_{l,i}^d$ are combined to get the final semantic embedding a_s . Classification loss L_g and L_s , and diversity loss L_{div} are leveraged for optimization. Note that shared layers in Backbone are frozen during training.

2.2 Generalization Branch: GNet

GNet aims to extract features easily generalized to unseen classes rather than those reflecting subtle differences in seen classes. Given an input image x , Backbone Net (i.e., ResNet101 [He *et al.*, 2016] in our experiments) embeds x to a visual embedding e_g , and the predictor f_g further projects e_g into the semantic space as a_g . GNet is optimized by the attribute-incorporated CrossEntropy loss \mathcal{L}_g to improve the compatibility between a_g and its true attribute:

$$\mathcal{L}_g = \text{CrossEntropy}(a_g, y) = -\log \frac{\exp(a_g^T \phi(y))}{\sum_{\hat{y} \in Y^S} \exp(a_g^T \phi(\hat{y}))} \quad (1)$$

where y denotes the label of x ; $\phi(y)$ is the attribute of y .

In contrast to standard ZSL methods with direct-training strategy, we further improve the generalization capability of GNet and restrain overfitting towards seen classes following the idea of episodic meta-learning [Finn *et al.*, 2017]. In detail, we first train GNet for adequate epochs to provide a preliminary classification ability and then freeze the Backbone Net and train f_g in an episode-wise manner.

In each episode, we sample batches of tasks. Each task contains a training set D_{tr}^j and a validation set D_{val}^j . Their samples belong to two disjoint class sets Y_{tr}^j and Y_{val}^j , respectively ($Y_{tr}^j, Y_{val}^j \subseteq Y^S$). We first use D_{tr}^j to virtually optimize f_g to get a virtual parameter $\theta'_g(D_{tr}^j)$, and then we minimize the cumulative validation loss of D_{val}^j calculated

based on virtual f_g to truly update f_g as follows:

$$\theta'_g(D_{tr}^j) \leftarrow \theta_g - \alpha \nabla_{\theta_g} \mathcal{L}_{\mathcal{D}_{tr}^j}^g(\theta_g) \quad (2)$$

$$\theta_g^* \leftarrow \theta_g - \beta \sum_j \nabla_{\theta_g} \mathcal{L}_{\mathcal{D}_{val}^j}^g(\theta'_g(D_{tr}^j)) \quad (3)$$

where $\theta'_g(D_{tr}^j)$ are the virtual parameters of f_g ; θ_g^* are the updated parameters; α and β are learning rates.

2.3 Balanced Specialization Branch: BSNet

The features learned by GNet may be too generalized and thus may not be sufficient to classify similar images, especially those from fine-grained datasets. To improve the specialization ability of our model, we propose the BSNet focusing on capturing discriminative features.

As shown in Figure 1, BSNet is composed of N sub-modules BSN_i , where $i \in [1, N]$. BSN_i first projects the input image into visual embeddings $e_{l,i}$. To save computation cost, we split the Backbone Net into two parts: shared layers and tail layers (we use the last nine convolutional layers and the pooling layer as tails in our experiments). The shared layers are frozen during training. Only tail layers are optimized. Instance- and dataset-level balance are then performed.

Instance-level Balance

For each sub-module, the instance-level balance generator $f_{b,i}$ takes $e_{l,i}$ and e_g as inputs, evaluates the generalization and specialization preference when classifying a specific image, and yields instance-level weights w_i^t . Specifically, the instance-weighted embedding $e_{l,i}^t$ is obtained by:

$$e_{l,i}^t = w_i^t \otimes e_{l,i} = f_{b,i}(e_{l,i}, e_g) \otimes e_{l,i} \quad (4)$$

where $e_{l,i} \in R^{1 \times K}$, $w_i^t \in (0, 1)^{1 \times K}$, and K is the channel number; \otimes indicates a channel-wise product.

w_i^t have two functions: 1) serving as an attention layer, allowing BSN_i to focus on important parts and then improve the specialization ability; 2) balancing the generalization (GNet) and specialization (BSNet) abilities by adjusting the weights of BSN_i .

Realizing the functions requires: (I) BSNet learns novel and discriminative knowledge that GNet cannot capture. Then, for a sub-module BSN_i , w_i^t should follow a distribution that: most of the weights are close to 0, and weights of special information are close to 1. In this way, we can reduce redundancy, strengthen unique visual information, and balance e_g and $e_{l,i}$ by adjusting $e_{l,i}$ with w_i^t . (II) For the first function, we further expect that w_i^t of different sub-modules $\{BSN_i\}_1^N$ focus on different aspects, i.e., for the k^{th} channel ($k \in [1, K]$), the weights are diverse across sub-modules. Then Requirement I can be extended to: for k^{th} channel, most sub-modules have $w_{i,k}^t$ close to 0, and only sub-modules attending this channel have weights near 1. Intuitively, the divergent distribution across different w_i^t enriches the diversity of specialization and thus facilitates classification.

Therefore, we propose a diversity loss \mathcal{L}_{div} to realize the functions and meet the requirements as follows:

$$\mathcal{L}_{div} = \sum_{k \in [1, K]} \sum_{i \in [1, N]} [w_{i,k}^t \hat{w}_{i,k}^t - mrg_k(w_{i,k}^t + \hat{w}_{i,k}^t)] \quad (5)$$

where $\hat{w}_{i,k}^t = \max_{i \neq n} w_{n,k}^t$ denotes the maximum value of other weights at k^{th} channel and mrg_k is a self-calculated margin for k^{th} channel.

\mathcal{L}_{dis} first accumulates the channel-wise loss and then the module-wise loss. Therefore, for each channel, we can sort $w_{i,k}^t$ to have the ordered weights without influencing the loss calculation: $w_k^t = \{w_{1,k}^t \leq w_{2,k}^t \leq \dots \leq w_{N,k}^t\}$. When calculating divergence loss for $w_{i,k}^t$, it will propagate gradients to $w_{i,k}^t$ and $\hat{w}_{i,k}^t$. Therefore, each calculation of instance-level divergence loss will produce a pair of gradients as follows:

$$\nabla \mathcal{L}_{div}(w_{i,k}^t)_{w_{i,k}^t} = \hat{w}_{i,k}^t - mrg_k \quad (6)$$

$$\nabla \mathcal{L}_{div}(w_{i,k}^t)_{\hat{w}_{i,k}^t} = w_{i,k}^t - mrg_k \quad (7)$$

where $\nabla \mathcal{L}_{div}(w_{i,k}^t)_{w_{i,k}^t}$ and $\nabla \mathcal{L}_{div}(w_{i,k}^t)_{\hat{w}_{i,k}^t}$ denote the gradients propagated to optimize $w_{i,k}^t$ and $\hat{w}_{i,k}^t$, respectively.

Then we can summarize gradients of $\mathcal{L}_{div}(w_k^t)$ as follows:

$$\nabla \mathcal{L}_{div}(w_k^t)_{w_{i,k}^t} = w_{N,k}^t - mrg_k \quad (i \in [1, N-2]) \quad (8)$$

$$\nabla \mathcal{L}_{div}(w_k^t)_{w_{N-1,k}^t} = 2 * (w_{N,k}^t - mrg_k) \quad (9)$$

$$\nabla \mathcal{L}_{div}(w_k^t)_{w_{N,k}^t} = \sum_{i=1}^{N-1} w_{i,k}^t + w_{N-1,k}^t - N * mrg_k \quad (10)$$

where $N \geq 3$, otherwise only Equations 9-10 are established.

From the above equations, we can easily find that:

$$\nabla \mathcal{L}_{div}(w_k^t)_{w_{i,k}^t} \propto w_{N,k}^t - mrg_k \quad (i \in [1, N-1]) \quad (11)$$

$$\nabla \mathcal{L}_{div}(w_k^t)_{w_{N,k}^t} \leq N * (\bar{w}_k^t - mrg_k) \propto \bar{w}_k^t - mrg_k \quad (12)$$

where \bar{w}_k^t is the mean value of weights w_k^t in the k^{th} channel.

To meet the two requirements, we want to optimize most weights (i.e., $\{w_{i,k}^t\}_1^{N-1}$) towards 0, and $w_{N,k}^t$ towards 1. Therefore, we need $\nabla \mathcal{L}_{div}(w_k^t)_{w_{i,k}^t} > 0$ and $\nabla \mathcal{L}_{div}(w_k^t)_{w_{N,k}^t} < 0$. Then, the upper and lower bounds of mrg_k to realize our goal are as follows:

$$mrg_k \in (\bar{w}_k^t, w_{N,k}^t) \quad (13)$$

where \bar{w}_k^t , $w_{N,k}^t$ are the mean value and the largest weight in k^{th} channel. Note that mrg_k exists only if $w_{1,k}^t \neq w_{N,k}^t$ in the ordered k channel weights; otherwise $mrg_k \in \emptyset$. Therefore, we initialize the weights with different values.

Based on the bounds, we design self-calculated mrg_k as:

$$mrg_k = \max(\bar{w}_k^t + \epsilon, (1 - \frac{1}{1 + eph})w_{N,k}^t) \quad (14)$$

where ϵ is a small value (e.g., $1e^{-6}$) to meet the lower bound (we add ϵ only when $\bar{w}_k^t + \epsilon < w_{N,k}^t$); eph is the epoch index.

During training, at the early stage when eph is small, mrg_k tends to be near the lower boundary. \mathcal{L}_{div} will decrease most weights to 0. As eph increases, mrg_k approaches the upper boundary. \mathcal{L}_{div} increases weights of important channels to 1. With this channel-wise self-calculated margin, \mathcal{L}_{div} in Eq. 5 can reduce redundancy and increase diversity.

Dataset-level Balance

This part aims to balance GNet and BSNet at dataset level and searches the best structure of BSNet according to dataset characteristics, e.g, fine-grained or coarse-grained. Given $e_{l,i}^t$, the balanced embedding $e_{l,i}^d$ is obtained by (adapted from HAT [Serra *et al.*, 2018]):

$$e_{l,i}^d = e_{l,i}^t \otimes \bar{w}_i^d = e_{l,i}^t \otimes \text{Sigmoid}(s * w_i^d) \quad (15)$$

where w_i^d is a parameterized dataset-level weight and is differentiable. *Sigmoid* activates w_i^d to fall into (0,1), and s is used as a scaling factor to adjust its sharpness. During training, s is calculated in a linear annealing schedule:

$$s = \textcircled{A}(eph) = \frac{1}{s_{max}} + (s_{max} - \frac{1}{s_{max}}) * \frac{eph - 1}{eph_{max} - 1} \quad (16)$$

where $s_{max} \gg 1$ is a hyper-parameter controlling the annealing schedule; eph_{max} is a pre-defined maximum epoch.

At first, since $s_{max} \gg 1$, s is close to 0, allowing *Sigmoid* to activate w_i^d in a uniform way that s approximately equals to 0.5. As eph increases, s increases, and \bar{w}_i^d will be gradually binarized. This design has two benefits: 1) it avoids premature deactivation of BSN_i to allow fully training; 2) the final binarized weight \bar{w}_i^d can be regarded as an approximate pruning of BSNet, i.e., it finds the approximately best structure for BSNet. Compared with using NAS to find optimal network, our design needs almost no extra computations.

Training objectives of BSNet. After passing through visual extraction, instance- and dataset-level balance in BSN_i , weighted embeddings $\{e_{l,i}^d\}_1^N$ are concatenated as $e_s \in R^{N \times K}$ and fed into the overall predictor f_s to get the specialized semantic embedding a_s : $a_s = f_s(e_s)$. We adopt classification loss \mathcal{L}_s to improve the semantic compatibility:

$$\mathcal{L}_s = \text{CrossEntropy}(a_s, y) = -\log \frac{\exp(a_s^T \phi(y))}{\sum_{\hat{y} \in Y^S} \exp(a_s^T \phi(\hat{y}))}$$

We train BSNet including all sub-modules $\{BSN_i\}_1^K$ and f_s simultaneously with the following objective function:

$$\mathcal{L}_{BSNet} = \mathcal{L}_s + \eta \mathcal{L}_{div} \quad (17)$$

where η is a hyper-parameter.

2.4 Training and Inference

Training. We first fine-tune the Backbone Net, and then freeze the Backbone and optimize GNet and BSNet separately. GNet is optimized in a meta-manner. For BSNet, we design two training strategies: *Parallel*, which trains instance- and dataset-level balance simultaneously, and *Sequential*, which excludes instance-level at first to train BSNet with only dataset-level balance for eph_{max} epochs, and then includes instance-level balance to train the whole BSNet. Training in parallel can encourage instance- and dataset-level weight to cooperate better. But gradients of *Sigmoid* function is unstable due to the schedule of s . Thus training sequentially can avoid that optimization of dataset-level balance impairs the optimization of instance-level balance.

Inference. We use the fusion of the generalized and specialized predictions for inference: $\bar{a} = a_g + a_s$. For ZSL, given an image x , we take the class with the highest fusion compatibility as the final prediction: $y^U = \arg \max_{c \in Y^U} \bar{a}^T \phi(c)$. For GZSL, to eliminate the bias towards seen classes, we adopt Calibrated Stacking (CS) [Chao *et al.*, 2016] to minus the confidence of seen classes by a pre-defined constant δ . The final prediction is: $y^{U \cup S} = \arg \max_{c \in Y^U \cup Y^S} \bar{a}^T \phi(c) - \delta$. Note that we set $s = s_{max}$ for inference, i.e., we use the approximately pruned BSNet.

3 Experiment

We evaluate our model on four widely-used benchmark datasets: SUN [Patterson and Hays, 2012], CUB [Welinder *et al.*, 2010], aPY [Farhadi *et al.*, 2009], and Awa2 [Xian *et al.*, 2019a]. SUN and CUB are fine-grained datasets, which may have high demand for specialization ability. SUN consists of 14,340 images from 717 scene classes with 102 attributes. CUB contains 11,788 images from 200 bird species with 312 attributes. aPY and Awa2 are coarse-grained datasets, comprising 15,339 images from 32 classes with 64 attributes, and 37,322 images from 50 diverse animals with 85 attributes, respectively. We adopt Proposed Split (PS) [Xian *et al.*, 2019a] to split datasets into seen and unseen classes for all methods.

All compared methods use ResNet101 as backbone or use ResNet101-extracted 2048D features as visual embeddings. As such, we use ResNet101 as our Backbone Net, and last 9 layers of ResNet101 as tail layers for BSNet. f_g , $f_{b,i}$, and f_s consist of one or two fully-connected layers. w_i^d are randomly-initialized parameters that have gradients and can be optimized. We sample data in 10-way, 5-shot, and 3-query for episodic-training of GNet. For BSNet, we set sub-module number $N = 10$, scaling factor $s_{max} = 5$, and max epoch $eph_{max} = 100$. More details are given in Appendix.

3.1 Comparisons with SOTA

We compare BGSNet with 14 state-of-the-art methods for both ZSL and GZSL settings. Our method is an end-to-end model focusing on improving image representation. It is fair to compare with other end-to-end methods. But to comprehensively review our performance gain, we further compare it with other generation methods and discriminative methods.

For **ZSL**, we adopt the average per-class Top-1 (T) accuracy for evaluation. As shown in Table 1, BGSNet achieves comparable or better results than SOTA on all datasets and consistently outperforms other end-to-end methods by a large margin (2.4%, 1.8%, 4.6%, and 0.3% improvements on SUN, CUB, aPY and Awa2, respectively). It indicates that BGSNet can learn image representations that generalize better to unseen classes and contain more discriminative information.

For **GZSL**, we evaluate the methods with T accuracy of seen classes (U), unseen classes (S), and their harmonic mean ($H = \frac{2US}{U+S}$). Among them, H is the key criteria considering both seen and unseen classes. From Table 1, we can find that our model achieves impressive gains compared to its end-to-end counterparts for H : 1.4%, 2.8%, and 2.8% on SUN, aPY, and Awa2 respectively, and obtains second-best result on CUB. The results prove that BGSNet can well balance

Method	ZSL				GZSL											
	SUN	CUB	aPY	AwA2	SUN			CUB			aPY			AwA2		
	T	T	T	T	U	S	H	U	S	H	U	S	H	U	S	H
TCN [Jiang <i>et al.</i> , 2019]	61.5	59.5	38.9	71.2	31.2	37.3	34.0	52.6	52.0	52.3	24.1	64.0	35.1	61.2	65.8	63.4
PREN [Ye and Guo, 2019]	60.1	61.4	-	66.6	35.4	27.2	30.8	35.2	55.8	43.1	-	-	-	32.4	88.6	47.4
PQZSL [Li <i>et al.</i> , 2019]	-	-	-	-	35.1	35.3	35.2	43.2	51.4	46.9	27.9	64.1	38.8	31.7	70.9	43.8
*LFGAA [Liu <i>et al.</i> , 2019]	61.5	67.6	-	68.1	20.8	34.9	26.1	43.4	79.6	56.2	-	-	-	50.0	90.3	64.4
*SGMA [Zhu <i>et al.</i> , 2019]	-	71.0	-	68.8	-	-	-	36.7	71.3	48.5	-	-	-	37.6	87.1	52.5
*AREN [Xie <i>et al.</i> , 2019]	60.6	71.5	39.2	67.9	40.3	32.3	35.9	63.2	69.0	66.0	30.0	47.9	36.9	54.7	79.1	64.7
TVN [Zhang <i>et al.</i> , 2019]	59.3	54.9	40.9	68.8	22.2	38.3	28.1	26.5	62.3	37.2	16.1	66.9	25.9	27.0	67.9	38.6
Zero-VAE-GAN [Gao <i>et al.</i> , 2020]	58.5	51.1	34.9	66.2	44.4	30.9	36.5	41.1	48.5	44.4	30.8	37.5	33.8	56.2	71.7	63.0
*VSG-CNN [Geng <i>et al.</i> , 2020]	-	-	-	-	30.3	31.6	30.9	52.6	62.1	57.0	22.9	66.1	34.0	60.4	75.1	67.0
*APN [Xu <i>et al.</i> , 2020]	60.9	71.5	-	68.4	41.9	34.0	37.6	65.3	69.3	67.2	-	-	-	56.5	78.0	65.5
*DAZLE [Huynh and Elhamifar, 2020]	59.4	66.0	-	67.9	24.3	52.3	33.2	59.6	56.7	58.1	-	-	-	75.7	60.3	67.1
*MIANet [Zhang <i>et al.</i> , 2021]	60.5	57.9	41.2	69.0	22.2	35.6	27.4	33.3	49.5	39.9	27.6	55.8	37.0	43.7	70.2	53.3
AMAZ [Li <i>et al.</i> , 2021]	60.7	68.9	-	68.2	42.0	35.1	38.3	58.2	55.7	56.9	-	-	-	60.1	69.2	64.3
SCILM [Ji <i>et al.</i> , 2021]	62.4	52.3	38.4	71.2	24.8	32.6	28.2	24.5	54.9	33.8	22.8	62.7	33.4	48.9	77.8	60.1
Ours *BGSNet	63.9	73.3	43.8	69.1	45.2	34.3	39.0	60.9	73.6	66.7	31.0	51.9	39.7	61.0	81.8	69.9

Table 1: Main experiments. * indicates end-to-end methods or methods using fine-tuned ResNet-101 as backbones. Best results are in bold.

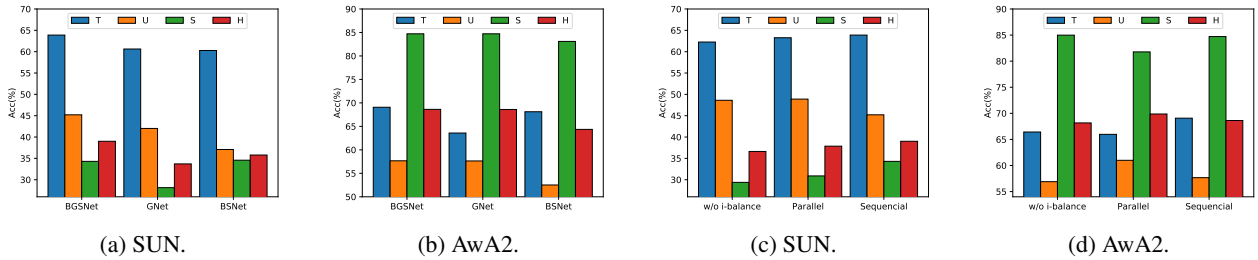


Figure 2: Ablation study. (a)-(b) Ablations of network modules. (c)-(d) Ablations of instance-level balance and training styles.

the generalization and specialization abilities, e.g., reducing specialization ability when transferring knowledge to unseen classes by decreasing weights of BSNet, or vice versa.

3.2 Ablation Study

Necessity of Two Branches: GNet and BSNet. We compare BGSNet (trained in *Sequential*) with its two branches: GNet and BSNet, each focusing only on generalization or specialization abilities. Figures 2 (a)-(b) shows the results. We can observe that BGSNet outperforms GNet and BSNet for both ZSL and GZSL, indicating that combining GNet and BSNet can improve the model’s adaptability to unseen classes and discernment of seen classes. We also find that GNet always outperforms BSNet in *U*, consistent with our expectation that generalization is more critical when classifying unseen classes. However, BSNet is not always superior to GNet in *S*. One possible reason is that we use L_{div} to restrict BSNet only to learn novel knowledge ignored by GNet, and thus BSNet may lack some basic knowledge for classification. More results on CUB and aPY are given in *Appendix*.

Benefits of Instance-level Balance. We then evaluate the effects of the instance-level balance. We compare BGSNet with its variant without instance-level balance and the variants that adopt different training strategies. Figures 2 (c)-(d) report the results. We find that variant without instance-

level balance obtains the worst performance on most datasets for both settings. The reason lies in that, without instance-level balance, BGSNet relies only on dataset-level balance to weigh GNet and BSNet, which is not as sufficient and suitable for a specific image as instance-level balance. Besides, our proposed L_{div} can optimize BSNet to capture novel knowledge neglected by GNet, and improve specialization diversity. As such, the absence of L_{div} also impairs the performance.

Comparing two training strategies, we observe that *Sequential* perform better than *Parallel* on SUN while worse on AwA2 for GZSL. This may be caused by the dataset characteristics. As discussed in Section 2.4, training in parallel results in better-cooperated instance- and dataset-level balance and unstable optimization of BSNet. The unstable optimization may impair its specialization ability, proved by *Sequential*’s superiority over *Parallel* in *S*. AwA2 is dataset with highly diverse classes and thus may have higher balance demands, while SUN needs specialization ability more as it contains highly similar classes. More ablations on other datasets and BGSNet’s variants are given in *Appendix*.

Benifits of Dataset-level Balance. We compare BGSNet with variant without dataset-level balance and variant without linear annealing. As shown in Figure 3 (a), including dataset-level balance improves the performance of both BGSNet and BSNet. Dataset-level balance can enhance important sub-

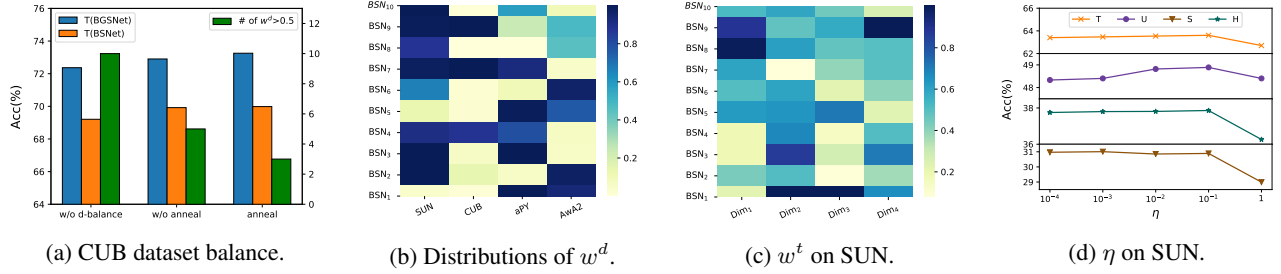


Figure 3: Balance analysis. (a)-(b) Ablation of dataset-level balance. (c)-(d) Analysis of instance-level balance.

modules by generating dataset-specific weights, and thus benefits BSNet, and better weighs GNet and BSNet. We also report the number of sub-modules with $w_i^d > 0.5$, and find that the annealing schedule can effectively reduce required sub-modules. BSNet and BGSNet even perform better with fewer sub-modules, demonstrating that dataset-level balancing in annealing schedule can find the optimal structure of BSNet.

3.3 Balance analysis

Dataset-level Balance. We draw the distribution of $\{w_i^d\}_1^N$ in Figure 3 (b). SUN needs most sub-modules in BSNet, indicating its high demand of specialization ability. However, another fine-grained dataset, CUB, needs fewer sub-modules than Awa2 and aPY. The reason may be that images in CUB are all about birds, and to discriminate birds, we only need to focus on a few areas such as wings, heads, bellies, etc.

Instance-level Balance on SUN. We randomly sample 4 dimensions from K channels of $\{w_i^t\}_1^K$ and draw their distribution in Figure 3 (c). The weights are diverse across sub-modules and channels, proving that our proposed diversity loss L_{div} can optimize the instance-level balance to meet our two requirements, and thereby, the two functions of w_i^t are fulfilled. We further vary ratio η of L_{div} and show results in Figure 3 (d). L_{div} is much larger than L_s . Thus the performance is stable when η is small and decreases when $\eta = 1$.

3.4 Hyper parameters

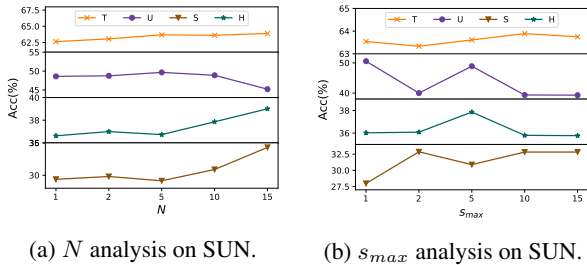


Figure 4: Hyper parameter analysis of BSNet.

We analyze BGSNet’s sensitivity to hyper-parameters, i.e., N and s_{max} . Figure 4 shows the results. The key criterion T and H increase as N increases, and achieves best results at 15 for SUN. The scaling factor s_{max} is best at 5. Analysis of other hyper-parameters and branches are given in Appendix.

4 Related Work

A typical solution to ZSL, called **discriminative methods**, is to project visual and semantic embeddings to a common space, and then perform nearest neighbor search in the space for classification. The common space can be the semantic [Ye and Guo, 2019; Li *et al.*, 2020], visual [Zhang *et al.*, 2017; Shen *et al.*, 2021], or a new latent space [Morgado and Vasconcelos, 2017; Jiang *et al.*, 2019]. For example, Li *et al.* [Li *et al.*, 2020] leverage the mutual information and entropy to learn modality-invariant embedding. TCN [Jiang *et al.*, 2019] designs a contrastive network to exploit the class similarities for robust embeddings.

Recently, some studies focus on **generation methods** to synthesize samples for unseen classes, converting ZSL to a traditional supervised learning problem [Gao *et al.*, 2020; Li *et al.*, 2021; Liu *et al.*, 2021]. Zero-VAE-GAN [Gao *et al.*, 2020] combines VAE and GAN to synthesize high-quality samples for unseen classes. Liu *et al.* [Liu *et al.*, 2021] propose to first align the distributions of visual embeddings belonging to the same task, and then generate samples based on the task-aligned embedding.

More related to our models are **end-end-to models**, which adopt backbone net, e.g., ResNet101, to learn image representation, and then based on the learned visual embeddings to perform classification by the discriminative strategy [Liu *et al.*, 2019; Xie *et al.*, 2019], or generative strategy [Xian *et al.*, 2019b; Zhang *et al.*, 2021]. For example, LFGAA [Liu *et al.*, 2019] integrate the backbone net with latent attribute attention to reduce semantic ambiguity. Our BGSNet adopts the discriminative strategy, and different from previous studies mainly in image representation learning. During the learning, our model equips both generalization and specialization abilities and balances the two abilities according to instance- and dataset-characteristics. However, most existing methods only focus on one of them, let alone balance them.

5 Conclusion

This paper proposes a novel BGSNet for zero-shot learning and generalized zero-shot learning. Unlike existing methods focusing only on either generalization or specialization, we develop two branches, i.e., GNet and BSNet, to learn transferable knowledge and extract discriminative features, respectively. The balance between the two branches is accomplished at instance- and dataset-level. The instance-level balance is optimized by the newly proposed diversity loss to

reduce redundancy and improve diversity across sub-modules of BSNet. In addition, the dataset-level balance can also play the role of network architecture searching to find optimal dataset-specific structures for BSNet. Extensive experiments show the effectiveness and explainability of our proposed methods in differentiating images and balancing the specialization and generalization abilities based on the instance and dataset types. In the future, we plan to extend our method in more real world applications that may suffer from the imbalanced network learning abilities, e.g., human activity recognition and natural language processing.

References

- [Chao *et al.*, 2016] Wei-Lun Chao, Soravit Changpinyo, Boqing Gong, and Fei Sha. An empirical study and analysis of generalized zero-shot learning for object recognition in the wild. In *ECCV*, pages 52–68. Springer, 2016.
- [Farhadi *et al.*, 2009] Ali Farhadi, Ian Endres, Derek Hoiem, and David Forsyth. Describing objects by their attributes. In *CVPR*, pages 1778–1785. IEEE, 2009.
- [Finn *et al.*, 2017] Chelsea Finn, Pieter Abbeel, and Sergey Levine. Model-agnostic meta-learning for fast adaptation of deep networks. In *ICML*, 2017.
- [Gao *et al.*, 2020] Rui Gao, Xingsong Hou, Jie Qin, Jiaxin Chen, Li Liu, Fan Zhu, Zhao Zhang, and Ling Shao. Zero-vae-gan: Generating unseen features for generalized and transductive zero-shot learning. *TIP*, 29, 2020.
- [Geng *et al.*, 2020] Chuanxing Geng, Lue Tao, and Songcan Chen. Guided cnn for generalized zero-shot and open-set recognition using visual and semantic prototypes. *Pattern Recognition*, 102:107263, 2020.
- [He *et al.*, 2016] Kaiming He, Xiangyu Zhang, Shaoqing Ren, and Jian Sun. Deep residual learning for image recognition. In *CVPR*, pages 770–778, 2016.
- [Huynh and Elhamifar, 2020] Dat Huynh and Ehsan Elhamifar. Fine-grained generalized zero-shot learning via dense attribute-based attention. In *CVPR*, 2020.
- [Ji *et al.*, 2021] Zhong Ji, Xuejie Yu, Yunlong Yu, Yanwei Pang, and Zhongfei Zhang. Semantic-guided class-imbalance learning model for zero-shot image classification. *IEEE Transactions on Cybernetics*, 2021.
- [Jiang *et al.*, 2019] Huajie Jiang, Ruiping Wang, Shiguang Shan, and Xilin Chen. Transferable contrastive network for generalized zero-shot learning. In *ICCV*, 2019.
- [Li *et al.*, 2019] Jin Li, Xuguang Lan, Yang Liu, Le Wang, and Nanning Zheng. Compressing unknown images with product quantizer for efficient zero-shot classification. In *CVPR*, pages 5463–5472, 2019.
- [Li *et al.*, 2020] Jingjing Li, Mengmeng Jing, Lei Zhu, Zhengming Ding, Ke Lu, and Yang Yang. Learning modality-invariant latent representations for generalized zero-shot learning. In *MM*, pages 1348–1356, 2020.
- [Li *et al.*, 2021] Yun Li, Zhe Liu, Lina Yao, and Xiaojun Chang. Attribute-modulated generative meta learning for zero-shot learning. *TMM*, pages 1–1, 2021.
- [Liu *et al.*, 2019] Yang Liu, Jishun Guo, Deng Cai, and Xiaofei He. Attribute attention for semantic disambiguation in zero-shot learning. In *ICCV*, October 2019.
- [Liu *et al.*, 2021] Zhe Liu, Yun Li, Lina Yao, Xianzhi Wang, and Guodong Long. Task aligned generative meta-learning for zero-shot learning. In *AAAI*, 2021.
- [Min *et al.*, 2020] Shaobo Min, Hantao Yao, Hongtao Xie, Zheng-Jun Zha, and Yongdong Zhang. Domain-oriented semantic embedding for zero-shot learning. *TMM*, 2020.
- [Morgado and Vasconcelos, 2017] Pedro Morgado and Nuno Vasconcelos. Semantically consistent regularization for zero-shot recognition. In *CVPR*, 2017.
- [Patterson and Hays, 2012] Genevieve Patterson and James Hays. Sun attribute database: Discovering, annotating, and recognizing scene attributes. In *CVPR*. IEEE, 2012.
- [Serra *et al.*, 2018] Joan Serra, Didac Suris, Marius Miron, and Alexandros Karatzoglou. Overcoming catastrophic forgetting with hard attention to the task. In *ICML*, 2018.
- [Shen *et al.*, 2021] Jiayi Shen, Zehao Xiao, Xiantong Zhen, and Lei Zhang. Spherical zero-shot learning. *TCSVT*, 2021.
- [Welinder *et al.*, 2010] Peter Welinder, Steve Branson, Takeshi Mita, Catherine Wah, Florian Schroff, Serge Belongie, and Pietro Perona. Caltech-ucsd birds 200. 2010.
- [Xian *et al.*, 2019a] Y Xian, CH Lampert, B Schiele, and Z Akata. Zero-shot learning—a comprehensive evaluation of the good, the bad and the ugly. *TPAMI*, 2019.
- [Xian *et al.*, 2019b] Yongqin Xian, Saurabh Sharma, Bernt Schiele, and Zeynep Akata. f-vae-gan-d2: A feature generating framework for any-shot learning. In *CVPR*, 2019.
- [Xie *et al.*, 2019] Guo-Sen Xie, Li Liu, Xiaobo Jin, Fan Zhu, Zheng Zhang, Jie Qin, Yazhou Yao, and Ling Shao. Attentive region embedding network for zero-shot learning. In *CVPR*, pages 9384–9393, 2019.
- [Xu *et al.*, 2020] Wenjia Xu, Yongqin Xian, Jiuniu Wang, Bernt Schiele, and Zeynep Akata. Attribute prototype network for zero-shot learning. In *NeurIPS*, 2020.
- [Yan *et al.*, 2021] Caixia Yan, Xiaojun Chang, Zhihui Li, Weili Guan, Zongyuan Ge, Lei Zhu, and Qinghua Zheng. Zeronas: Differentiable generative adversarial networks search for zero-shot learning. *TPAMI*, 2021.
- [Ye and Guo, 2019] Meng Ye and Yuhong Guo. Progressive ensemble networks for zero-shot recognition. In *CVPR*, pages 11728–11736, 2019.
- [Zhang *et al.*, 2017] Li Zhang, Tao Xiang, and Shaogang Gong. Learning a deep embedding model for zero-shot learning. In *CVPR*, pages 2021–2030, 2017.
- [Zhang *et al.*, 2019] Haofeng Zhang, Yang Long, Yu Guan, and Ling Shao. Triple verification network for generalized zero-shot learning. *TIP*, 28(1):506–517, 2019.

- [Zhang *et al.*, 2021] Haofeng Zhang, Yinduo Wang, Yang Long, Longzhi Yang, and Ling Shao. Modality independent adversarial network for generalized zero shot image classification. *Neural Networks*, 134:11–22, 2021.
- [Zhu *et al.*, 2019] Yizhe Zhu, Jianwen Xie, Zhiqiang Tang, Xi Peng, and Ahmed Elgammal. Semantic-guided multi-attention localization for zero-shot learning. In *NeurIPS*, pages 14943–14953, 2019.